INORGANIC CHEMISTRY







FRONTIERS

RESEARCH ARTICLE

View Article Online
View Journal | View Issue



Cite this: *Inorg. Chem. Front.*, 2024, **11**, 1890

Partial substitution with a significant effect: coexistence of a wide band gap and large birefringence in the oxychalcogenide AEGe₂O₄Se (AE = Sr and Ba)†

Mao-Yin Ran, a,b,c Sheng-Hua Zhou, a,b,c Wen-Bo Wei, a,b,c A-Yang Wang, a,b,d Xin-Tao Wu, a,b Hua Lin x,b and Qi-Long Zhu x,b +a,b

Much effort has been devoted to the discovery of novel birefringent crystals that display considerable birefringence (Δn) in the infrared (IR) region. However, the simultaneous achievement of a wide energy gap ($E_g > 3.1 \, \mathrm{eV}$) and a large Δn (>0.2) in a heteroanionic chalcogenide system remains a formidable challenge. To address this bottleneck, we applied the partial-substitution strategy and successfully designed and synthesized two new quaternary oxychalcogenides, namely AEGe₂O₄Se (AE = Sr and Ba). These two isomorphic compounds belong to the monoclinic space group $P2_1/c$ (no. 14), featuring a structure composed of two-dimensional (2D) $[\mathrm{Ge_2O_4Se}]^{2-}$ layers with an antiparallel arrangement, which are separated by charge-balanced Ba²⁺ cations. Remarkably, they exhibit the coexistence of large Δn values (0.209 and 0.238@2050 nm based on the generalized gradient approximation) and wide E_g values (3.57 and 3.81 eV). Furthermore, theoretical calculations were performed to elucidate the interplay between optical properties and electronic structures. These results reveal that the significantly improved Δn value (approximately 15–17 times that of the parent compound BaGe₂O₅) can mainly be attributed to the newly discovered [GeO₃Se] heteroanionic motif. In brief, this study provides a simple chemical substitution method to overcome the trade-off between wide E_g and large Δn values in heteroanionic chalcogenides.

Received 6th December 2023, Accepted 15th February 2024 DOI: 10.1039/d3qi02509h

rsc.li/frontiers-inorganic

Introduction

Birefringent crystals play an important role in the generation and manipulation of optical polarization, finding widespread applications in laser science and technology. They are particularly significant in optical communications, leading to continuous and comprehensive research efforts. Currently, commercial birefringent materials are primarily composed of oxides, such as YVO_4 , 2 $CaCO_3$, and BaB_2O_4 . Although these materials exhibit high birefringence (Δn), their application is limited to the ultraviolet and visible range due to the narrow transmission cut-off edge caused by the absorption vibrations

of metal-oxygen bonds. Consequently, they cannot be utilized

Chalcogenides are classical candidates for photoelectric functional materials in the IR region, with crystal structures predominantly composed of tetrahedral building units.6 However, the weak polarization anisotropy of these rigid building units often leads to smaller Δn , which limits their comprehensive application. During the past decade, several effective structural design strategies have been employed to address these issues,8 including: (1) introducing other groups containing lone-pair electrons, 9 (2) introducing π -conjugated units, 10 and (3) exploring new functional building units (FBUs) with significant anisotropy. 11 Although the strategies mentioned above have achieved some crystal materials with high Δn values, an ideal birefringent chalcogenide also needs to consider another key parameter: the transmission range. This parameter is typically dependent on the optical energy gap (E_g) of chalcogenides, which, in turn, determines the range of

in the infrared (IR) band. Moreover, the pursuit of materials capable of achieving a large Δn plays a critical role in advancing the miniaturization of optical devices.⁵ To meet the increasing demands for such materials in laser technology, there is an urgent need to develop new high-performance birefringent crystals, especially for the IR band.

^aState Key Laboratory of Structural Chemistry, Fujian Institute of Research on the Structure of Matter, Chinese Academy of Sciences, Fuzhou 350002, China. E-mail: linhua@fjirsm.ac.cn, qlzhu@fjirsm.ac.cn

^bFujian Science & Technology Innovation Laboratory for Optoelectronic Information of China, Fuzhou, Fujian 350108, China

^cUniversity of Chinese Academy of Sciences, Beijing 100049, China

^dCollege of Chemistry, Fuzhou University, Fujian 350002, China

[†] Electronic supplementary information (ESI) available: Additional experimental and theoretical results together with additional tables and figures. CCDC 2301111 and 2301112. For ESI and crystallographic data in CIF or other electronic format see DOI: https://doi.org/10.1039/d3qi02509h

applications for chalcogenides. However, the different requirements for the microstructure of materials due to large Δn and wide E_{σ} values make it difficult for these characteristics to coexist simultaneously in the same material. Therefore, how to effectively achieve a balance between large Δn (>0.2) and wide E_{σ} (>3.1 eV) values is currently a difficult and hot research topic in this system.

Oxychalcogenides containing heteroanionic groups have garnered significant attention as a noteworthy category of candidates for IR birefringent crystals. 12 They offer the synthesis of advantageous properties found in both oxides and chalcogenides. This system demonstrates flexible assembly methods and versatile optical performance. The presence of heteroanionic motifs within the structure not only retains the wide E_{o} value of the parent oxide but also exhibits a large anisotropic polarization index, contributing to the achievement of a high Δn value.¹³ For instance, the anisotropy of the heteroanionic [GeOS₃] motif is six times that of the tetrahedral [GeO₄] unit and twice that of the [GeS₄] unit.¹⁴ Furthermore, partially substituting oxygen in oxides with chalcogenide elements proves to be an effective approach for attaining oxychalcogenides with Δn values, ¹⁵ for example, (0.105@2050 nm, with the original structure being $Ba_2TiSi_2O_8$), ¹⁶ $Sr_3Ge_2O_4Te_3$ (0.152@2090 nm, with the original $Sr_2ZnGe_2O_7$, ¹⁷ structure being and Sr₂CdGe₂OS₆ (0.193@2050 with the original structure being Sr₂CdGe₂O₇).¹⁸

Recently, we have been focusing on the ternary $AE_xM_yO_{x+2y}$ (AE = alkaline-earth metals; M = group 14 elements) system, which displays a diverse range of constituents and phases. This system showcases structural flexibility, ranging from 0D clusters to 3D frameworks, achieved through simple changes in constituents. As a result, it holds potential for designing new oxychalcogenides. Among the various compounds in this system, AEGe₂O₅ has captured our attention. Despite its promising two-dimensional (2D) layered structure, which facilitates the attainment of larger Δn , the reality is quite the opposite (the theoretical Δn is much less than 0.02). This is primarily due to the rigid composition of its functional groups, namely tetrahedral [GeO₄] and octahedral [GeO₆]. Inspired by the aforementioned strategies, we implemented the partial-substitution approach and effectively devised and synthesized two novel quaternary oxychalcogenides, namely AEGe₂O₄Se (AE = Sr and Ba). This study encompasses the solid-phase synthesis, structural progression, and optical characteristics AEGe₂O₄Se (AE = Sr and Ba). Additionally, theoretical calculations were carried out to attain a more comprehensive understanding of the structure-activity relationship.

Results and discussion

BaGe₂O₅¹⁹ crystallizes in the orthorhombic *cmca* (no. 64) space group. Within its structure, the asymmetric unit comprises one independent Ba atom, two Ge atoms, and four O atoms. The basic structural units of BaGe₂O₅ can be visualized

as comprising [Ge1O₆] octahedra and [Ge2O₄] tetrahedra (as shown in Fig. 1a). The [Ge1O₆] octahedra connect along the b-axis to form an infinite chain (Fig. S1†) through cornersharing O atoms, and the remaining O atoms of the [Ge1O₆] octahedra link two [Ge2O4] tetrahedra along the b-axis direction to form a 2D layer (Fig. 1b) through edge-sharing O atoms. Ba²⁺ cations located in the interlayer (Fig. 1c) stabilize this structural configuration to maintain charge balance. Unfortunately, the highly symmetric polyhedral shapes resulting from the rigid coordination model limit polarization anisotropy, resulting in a relatively low Δn of BaGe₂O₅. It is important to note that the anisotropic polarizability within a material's structure directly affects its Δn property. Therefore, a flexible coordination environment is more favorable for enhancing Δn .²⁰ Accordingly, the pursuit of flexible FBUs, rather than rigid ones, is being considered as an effective strategy to increase Δn .

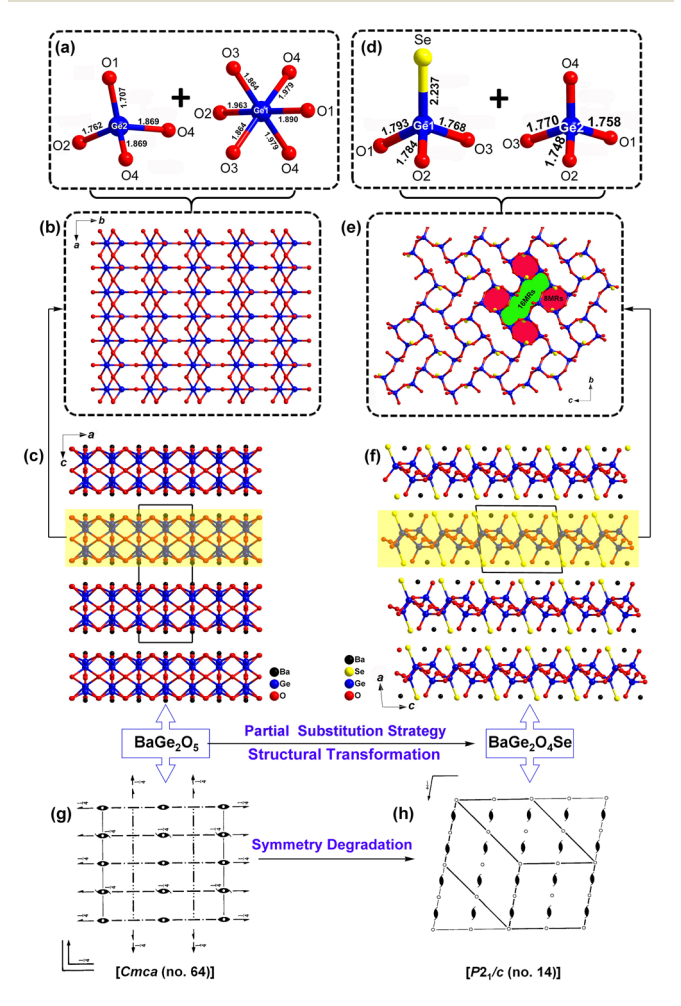


Fig. 1 Structural transformation from oxide BaGe₂O₅ to oxychalcogenide BaGe₂O₄Se: (a and d) coordination environment of [GeO₄], [GeO₆], and [GeO₃Se] units with the atom numbers outlined; (b and e) 2D $[Ge_2O_5]^{2-}$ and $[Ge_2O_4Se]^{2-}$ anion layers; (c and f) the 2D layered structures viewed from the b direction; (q and h) symmetry degradation from Cmca (no. 64) to P2₁/c (no. 14).

Oxyselenides, AEGe₂O₄Se (AE = Sr and Ba), represent novel quaternary compounds discovered in AE/M^{IV}/O/Q systems. Due to their isostructural nature, BaGe₂O₄Se is used as a representative compound to describe the crystal structure. BaGe₂O₄Se adopts the monoclinic P2₁/c (no.14) space group, and detailed crystallographic data information can be found in Table 1. The asymmetric unit contains one unique Ba atom, two Ge atoms, four O atoms, and one Se atom, all located at the Wyckoff site 4e. The fundamental structure of BaGe₂O₄Se consists of a 2D [Ge₂O₄Se]²⁻ layer, with Ba²⁺ cations filling the interlayer spaces to effectively balance the charge (Fig. 1f). The AE atoms are coordinated with five O atoms and three Se atoms to form [AEO₅Se₃] polyhedra (Fig. S2†). The coordination environment of Ge is depicted in Fig. 1d, and detailed bond lengths and bond angles can be found in Tables S1-S3.† The Ge2 atom is connected to four O atoms, forming [GeO4] FBUs with Ge-O bond lengths ranging from 1.748 to 1.770 Å. In contrast, the Ge1 atom is linked to three O atoms and one Se atom, forming highly polarized heteroanionic [GeO₃Se] FBUs with Ge-O bond lengths ranging from 1.768 to 1.784 Å and Ge-Se bond lengths of 2.237 Å. The structure further evolves as two [GeO₃Se] FBUs and two [GeO4] FBUs share edges to create larger building units known as [Ge₄O₈Se₂] 8-membered-rings (8MRs). These 8MRs interconnect, ultimately resulting in the formation of a two-dimensional [Ge₂O₄Se]²⁻ layer through corner-sharing (as illustrated in Fig. 1e). Within this layer, a [Ge₈O₁₆Se₄] 16MR is generated, nestled inside four closely situated [Ge₄O₈Se₂] 8MRs.

The detailed structural evolution from the oxide $BaGe_2O_5$ to the oxychalcogenide $BaGe_2O_4Se$ is depicted in Fig. 1. Both $BaGe_2O_5$ and $BaGe_2O_4Se$ exhibit a similar 2D layered structure. However, there are differences in their FBUs. $BaGe_2O_5$ contains $[GeO_6]$ and $[GeO_4]$ FBUs, and it is evident that these rigidly coordinated FBUs prohibit significant changes in Δn within the parent oxide $BaGe_2O_5$. By introducing Se atoms, which possess

Table 1 Crystal data and structural refinement details of $AEGe_2O_4Se$ (AE = Sr and Ba)

Empirical formula	SrGe ₂ O ₄ Se	BaGe ₂ O ₄ Se
CCDC	2301112	2301111
Formula weight	375.76	425.48
Temperature(K)	293(2)	293(2)
Crystal system	Monoclinic	Monoclinic
Space group	$P2_1/c$ (no. 14)	$P2_1/c$ (no. 14)
a (Å)	6.7668(4)	7.0948(3)
b (Å)	9.5262(5)	9.5602(3)
c (Å)	8.2232(5)	8.4161(3)
β (°)	95.729(5)	95.978(4)
$V(\mathring{A}^3)$	527.44(5)	567.74(4)
Z	4	4
$D_{\rm c} ({\rm g \cdot cm}^{-3})$	4.732	4.978
$\mu (\text{mm}^{-1})$	28.212	23.708
\overrightarrow{GOOF} on F^2	1.095	1.124
R_1 , w R_2 $(I > 2\sigma(I))^a$	0.0440, 0.1155	0.0294, 0.0864
R_1 , w R_2 (all data)	0.0480, 0.1175	0.0307, 0.0874
Largest diff. peak and hole $(e \cdot Å^{-3})$	1.23, -2.63	1.115, -2.151

 $^{^{}a}R_{1} = \sum ||F_{o}| - |F_{c}||/\sum |F_{o}|, wR_{2} = [\sum w(F_{o}^{2} - F_{c}^{2})^{2}/\sum w(F_{o}^{2})^{2}]^{1/2}.$

different electronegativity and size ($\chi_{\rm O}=3.44$ vs. $\chi_{\rm Se}=2.55$), structural modifications are achieved through a partial substitution strategy. In BaGe₂O₄Se, the inclusion of flexible coordinated [GeO₃Se] heteroanionic FBUs results in an increased Δn value, which is further supported by experimental observations and theoretical analyses as elaborated below. It is worth noting that in contrast to the previously reported approach of enhancing Δn through a dimensionality reduction strategy, this is the rare instance of improving Δn in an oxychalcogenide system with 2D structures.

Moreover, through a comprehensive comparison and analysis of previously known oxychalcogenides, we have found that AEGe₂O₄Se (AE = Sr and Ba) exhibits the uniqueness of the structure in three categories. Firstly, the distinguishing feature lies in four-coordinated anionic FBUs, denoted as $[GeO_xQ_{4-x}]^{21-27}$ This group can be systematically categorized into various subgroups, such as [GeQ₄], [GeOQ₃], [GeO₂Q₂], [GeO₃Q], and [GeO₄], depending on the variation of x. In comparative terms, the [GeOQ₃] anionic motif stands out as the most frequently observed, with reports of [GeOS₃],²² [GeOSe₃],²³ and [GeOTe₃],²⁴ respectively. The [GeO₂Q₂] FBUs have also been reported, further divided into subgroups like [GeO₂S₂]²⁵ and [GeO₂Se₂].²⁶ In contrast, [GeO₃Q] FBUs are relatively underrepresented, with the [GeO3S] FBU only being the primary instances found in some oxychalcogenides.27 Remarkably, prior to this research, no reports existed regarding the [GeO₃Se] and [GeO₃Te] FBUs. Our study has discovered, for the first time, the heteroanionic [GeO₃Se] FBU, thus enriching the diversity of oxychalcogenides. Additionally, we have also calculated the formation enthalpies of the title compounds,28 as well as the reported oxyselenides. As shown in Fig. S3,† the formation energies of SrGe₂O₄Se and BaGe₂O₄Se are -1.821 eV per atom and -1.832 eV per atom, respectively, which is even lower compared to most of the reported oxyselenides. This indicates that the title compounds are thermodynamically stable even under zero external pressure. The lack of previous discoveries in this area may be attributed to factors such as the choice of starting material, proportions, and the temperature program utilized in the reaction. Secondly, we have observed that the $[GeO_xQ_{4-x}]$ FBUs tend to exist largely independently within oxythiogermanate compounds. A notable exception to this trend is the compound $Ba_3M^{II}Ge_3O_2S_8$ (M^{II} = Mn, Cd), ²⁹ in which we have recently discovered the coexistence of [GeOS₃] and [GeO₂S₂]. This simultaneous presence of different motifs is a relatively rare phenomenon within the context of [GeO₄]/[GeQ₄] and $[GeO_xQ_{4-x}]$ FBUs. Additionally, we have uncovered another interesting occurrence where [GeO4] and [GeO3Se] FBUs are both present within the same structural framework. Thirdly, our research introduces the most oxygen-rich system within the realm of AE-M^{IV}-O-Q systems reported thus far. This system, namely AE-M2IV-O4-Q, offers a novel approach for designing wide energy gap oxychalcogenides.

 $AEGe_2O_4Se$ (AE = Sr and Ba) was synthesized through hightemperature solid-phase synthesis, using a stoichiometric ratio of AE (Sr and Ba), Se, and GeO_2 at 1223 K. Millimeter-sized single crystals were chosen for testing and characterization purposes. The powder XRD results were in agreement with the results obtained from single crystal test simulations, confirming the purity of the AEGe₂O₄Se (AE = Sr and Ba) phase (Fig. S4†). EDX elemental analysis demonstrated that the AE/ Ge/O/Se ratio was well consistent with the results based on the single crystal tests (Fig. S5 and S6†). Moreover, AEGe₂O₄Se (AE = Sr and Ba) exhibited excellent thermal stability under a N₂ atmosphere below 1100 K (Fig. S7†), as there were no observed melting or phase transition features in the corresponding TG-DTA curves. Furthermore, both SrGe₂O₄Se and BaGe₂O₄Se displayed a wide IR transmission cut-off edge at 13.3 and 13.5 µm, respectively (Fig. 2a and b), indicating their potential as birefringent materials for IR applications. It is apparent that there is a prominent absorption peak near 9 µm, which could be attributed to the multi-phonon absorption. A comparable occurrence has also been observed in the infrared transmission spectra of recently reported chalcogenides.³⁰ The optical Eg value of AEGe2O4Se was determined through UV-vis-NIR diffuse reflectance spectra. The calculated $E_{\rm g}$ values using the Kubelka-Munk function³¹ were found to be 3.57 and 3.81 eV for SrGe₂O₄Se and BaGe₂O₄Se, respectively (Fig. 2c and d).

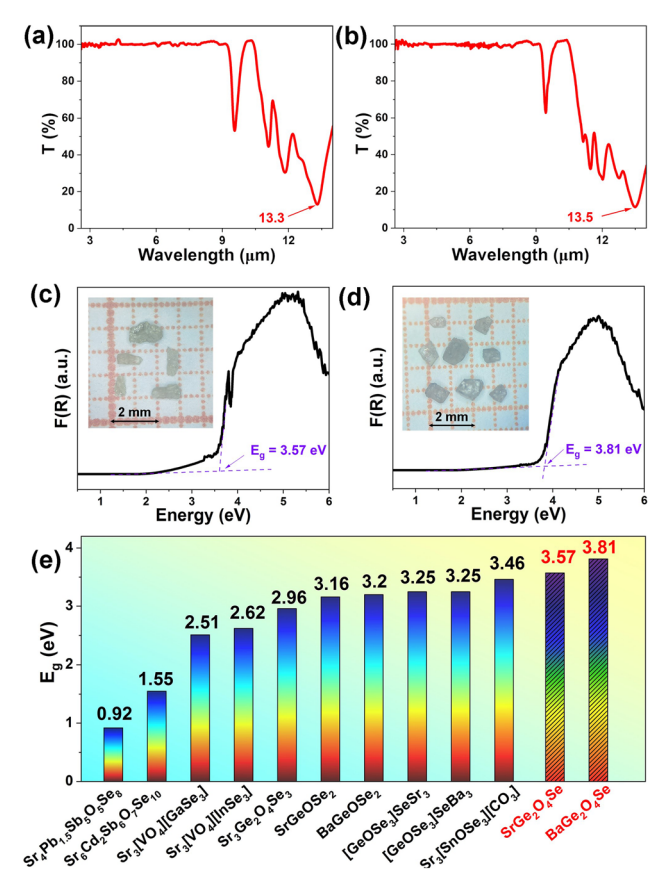


Fig. 2 Optical property characterization of AEGe₂O₄Se (AE = Sr and Ba): (a and b) IR transmittance spectra; (c and d) UV-vis-NIR absorption spectra (inset: photographs of crystals); (e) comparison of the experimental E_{α} value of reported oxyselenides.

Importantly, these values are the highest among all known oxyselenides (Fig. 2e).32

To determine the Δn values of AEGe₂O₄Se (AE = Sr and Ba) in our experiment, we performed Δn measurements on specific crystals based on a ZEISS Axio A1 cross-polarizing microscope equipped with a Berek compensator. For SrGe₂O₄Se, we found that the retardation (R-value) was 1.649 μm and the crystal thickness (T-value) was 10.37 μm. Similarly, for BaGe₂O₄Se, the corresponding values were determined to be 0.895 µm and 7.67 µm. According to the formula $\Delta n = R/T_1^{33}$ the measured Δn values for SrGe₂O₄Se and BaGe₂O₄Se were 0.16 and 0.12, respectively (Fig. 3). These Δn values are bigger than those of many commercial birefringent as MgF₂ (0.012@632 nm),³⁴ LiNbO₃ such $(0.08@632 \text{ nm})^{35}$ and BaB_2O_4 $(\Delta n = 0.122@546 \text{ nm})^4$ Additionally, they are also larger than those of several typical chalcogenides, including [Ba₄(S₂)][ZnGa₄S₁₀] (0.053@1064 nm),³⁶ $NaSrBS_3$ (0.137@546 nm), ³⁷ and $K_2Na_2Sn_3S_8$ (0.070@546 nm). ³⁸

To gain a comprehensive understanding of the electronic structure and optical properties of AEGe2O4Se (AE = Sr and Ba), we conducted detailed theoretical studies based on the DFT method. As displayed in Fig. 4a and b, AEGe₂O₄Se (AE = Sr and Ba) exhibits an indirect E_g with calculated values being 1.95 and 2.18 eV, respectively. These values are lower than the experimental results obtained from the solid-state spectra (3.57 and 3.81 eV). This deviation mainly stems from the limited accuracy of traditional DFT functions in E_g calculations.39 The partial density of states (PDOS) reveals that the valence band maximum (VBM) is predominantly influenced by Se-4p and O-2p orbitals, whereas the conduction band minimum (CBM) is mainly associated with the vacant Ge-3s

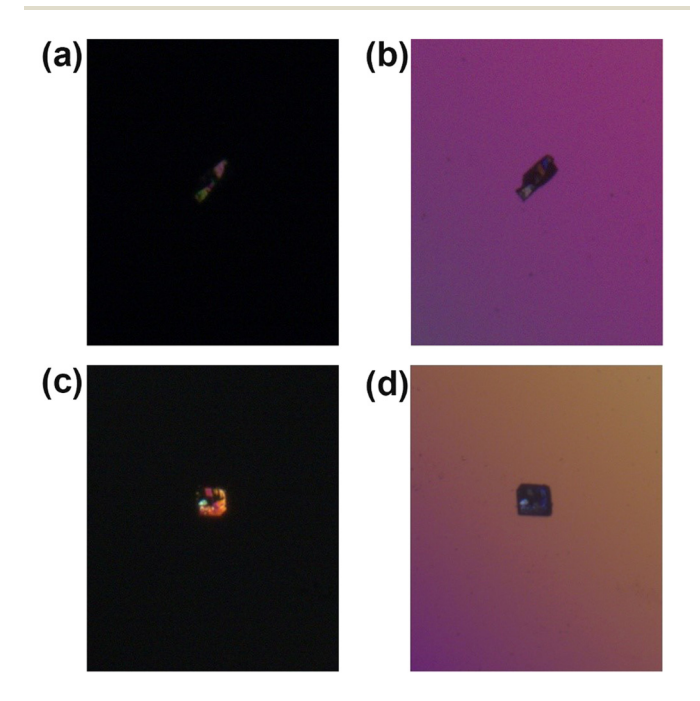


Fig. 3 Changes in the interference color of (a and b) SrGe₂O₄Se and (c and d) BaGe₂O₄Se crystals before and after complete extinction.

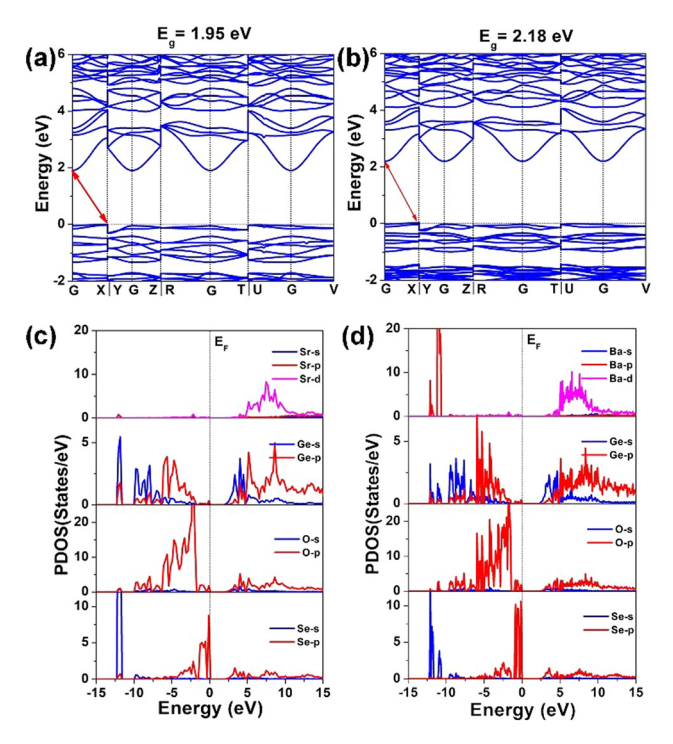


Fig. 4 Theoretical calculated results of AEGe₂O₄Se (AE = Sr and Ba): (a and b) electronic band structures and (c and d) PDOS curves.

and Ge-3p orbitals (Fig. 4c and d). The AE atoms make minimal contributions around the $E_{\rm F}$ and act as balanced charges to stabilize the 2D layered structure. Consequently, the E_g value of AEGe₂O₄Se (AE = Sr and Ba) is primarily influenced by the heteroanionic [GeO₃Se] FBUs, specifically the 2D $[Ge_2O_4Se]^{2-}$ layer.

Additionally, we employed the DFT method to calculate the Δn value of AEGe₂O₄Se (AE = Sr and Ba). The calculated results show Δn values of 0.238 and 0.209@2050 nm, and 0.241 and 0.212@1064 nm for SrGe₂O₄Se and BaGe₂O₄Se, respectively (Fig. 5a). The calculated values are larger than the measured Δn values due to the fact that only crystal wafers can be measured in a cross-polarizing microscope, resulting in smaller measured values than the Δn of the material. Furthermore, the parent $BaGe_2O_5$ exhibits a low Δn value of 0.014@2050 nm and 0.015@1064 nm. Notably, partial substitution is an effective strategy in designing birefringent materials with enhanced Δn values.

Based on the above discussion, AEGe₂O₄Se not only undergoes a structural transition from the parent BaGe₂O₅ but also exhibits excellent optical properties. These achievements can be attributed to the presence of heteroanionic [GeO₃Se] FBUs at two levels. In comparison with other reported oxychalcogenides (see Table S4† for details), a two-dimensional diagram (Fig. 5b) was plotted, showing the horizontal axis representing the "perfect area" in the graph (Δn) with values greater than 0.2 (representing most commercial materials) and the vertical axis (E_g) exceeds 3.1 eV (corresponding to the cut-off edge of the ultraviolet band at 400 nm). Notably, AEGe₂O₄Se (AE = Sr

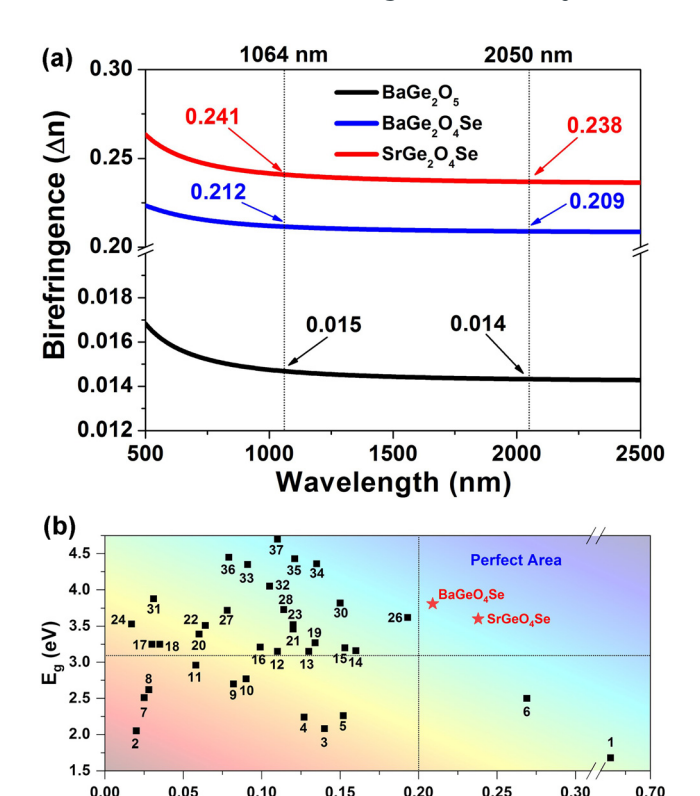


Fig. 5 (a) Calculated birefringence (Δn) of oxide BaGe₂O₅ and oxychalcogenide AEGe₂O₄Se (AE = Sr and Ba); (b) comparison of the experimental E_{q} and calculated Δn values of known oxychalcogenides (1–37) listed in Table S4.†

Birefringence (An)

and Ba) exhibits a coexistence of large calculated Δn values (0.209 and 0.238@2050 nm) and wide experimental $E_{\rm g}$ values (3.57 and 3.81 eV), indicating their potential as birefringent crystals in the ultraviolet-visible-infrared band.40

Conclusions

In summary, we have successfully discovered a new type of quaternary phase in the AE/MIV/O/Q system, namely AEGe₂O₄Se (AE = Sr and Ba), through a partial substitution strategy from the parent BaGe₂O₅. These structures feature a unique 2D [Ge₂O₄Se]²⁻ layer formed by the first discovered heteroanionic [GeO₃Se] motif. Comparing the structures of AEGe₂O₄Se (AE = Sr and Ba) a the parent BaGe₂O₅, similar layered structures but different FBUs have been observed, indicating a successful structural transformation and optimization achieved through partial Se substitution for O. Furthermore, AEGe₂O₄Se (AE = Sr and Ba) exhibits excellent optical properties, including a wide IR transparent region (13.3-13.5 μm), high Δn values (0.209–0.238@2050 nm) and large $E_{\rm g}$ values (3.57-3.81 eV). These properties suggest that AEGe₂O₄Se crystals hold promise as candidates for IR birefringent materials. Further investigation into the structure-property relationship reveals that the excellent birefringent properties can be attributed to the significant structural anisotropy of heteroanionic [GeO₃Se] groups. Overall, this work highlights the oxychalcogenide system as a promising source of IR birefringent crystals, presenting a new route for exploring IR birefringent crystals with well-balanced comprehensive properties.

Author contributions

Mao-Yin Ran: investigation, formal analysis, and writing original draft. Sheng-Hua Zhou: investigation, methodology, and validation. Wen-Bo Wei: formal analysis and validation. A-Yang Wang: formal analysis and validation. Xin-Tao Wu: conceptualization and writing - review & editing. Hua Lin: supervision, conceptualization, and writing - review & editing. Qi-Long Zhu: supervision and writing - review & editing.

Conflicts of interest

There are no conflicts to declare.

Acknowledgements

This research was supported by the National Natural Science Foundation of China (21771179), the Fujian Science & Technology Innovation Laboratory for Optoelectronic Information of China (2021ZR118), and the Natural Science Foundation of Fujian Province (2022L3092 and 2023H0041).

References

1 (a) Z. Xie, L. Sun, G. Han and Z. Gu, Optical Switching of a Birefringent Photonic Crystal, Adv. Mater., 2008, 20, 3601-3604; (b) N. Berti, S. Coen, M. Erkintalo and J. Fatome, Extreme waveform compression with a nonlinear temporal focusing mirror, Nat. Photonics, 2022, 16, 822-827; (c) Y. Zhou, X. Zhang, M. Hong, J. Luo and S. Zhao, Achieving effective balance between bandgap and birefringence by confining π -conjugation in an optically anisocrystal, *Sci.* Bull., 2022, 67, 2276–2279; (d) M. Mutailipu, J. Han, Z. Li, F. M. Li, J. J. Li, F. F. Zhang, X. F. Long, Z. H. Yang and S. L. Pan, Achieving the fullwavelength phase-matching for efficient nonlinear optical frequency conversion in C(NH₂)₃BF₄, Nat. Photonics, 2023, 17, 694-701; (e) F. Zhang, X. Chen, M. Zhang, W. Jin, S. Han, Z. Yang and S. Pan, An excellent deep-ultraviolet birefringent material based on [BO₂]_∞ infinite chains, Light: Sci. Appl., 2022, 11, 252; (f) X. Dong, L. Huang, H. Zeng, Z. Lin, K. M. Ok and G. Zou, High-Performance Sulfate Optical Materials Exhibiting Giant Second Harmonic Generation and Large Birefringence, Angew. Chem., Int. Ed., 2022, 61, e202116790; (g) P.-F. Li, C.-L. Hu, F. Kong and J.-G. Mao, The First UV Nonlinear Optical

- Selenite Material: Fluorination Control in CaYF(SeO₃)₂ and Y₃F(SeO₃)₄, Angew. Chem., Int. Ed., 2023, **62**, e202301420.
- 2 H. Luo, T. Tkaczyk, E. Dereniak and K. Oka, High birefringence of the yttrium vanadate crystal in the middle wavelength infrared, Opt. Lett., 2006, 31, 616-618.
- 3 G. Ghosh, Dispersion-equation coefficients for the refractive index and birefringence of calcite and quartz crystals, Opt. Commun., 1999, 163, 95-102.
- 4 G. Zhou, J. Xu, X. Chen, H. Zhong and F. Gan, Growth and spectrum of a novel birefringent α-BaB₂O₄ crystal, J. Cryst. Growth, 1998, 191, 517-519.
- 5 S. Niu, J. Graham, H. Zhao, Y. Zhou, O. Thomas, H. Huaixun, S. Jad, M. Krishnamurthy, U. Brittany and J. Wu, Giant optical anisotropy in a quasi-one-dimensional crystal, Nat. Photonics, 2018, 12, 392-396.
- 6 H. Chen, M. Y. Ran, W. B. Wei, X. T. Wu, H. Lin and Q. L. Zhu, A comprehensive review on metal chalcogenides with three-dimensional frameworks for infrared nonlinear optical applications, Coord. Chem. Rev., 2022, 470, 214706.
- 7 (a) M. Zhou, C. Li, X. Li, J. Yao and Y. Wu, K₂Sn₂ZnSe₆, Na₂Ge₂ZnSe₆, and Na₂In₂GeSe₆: A New Series of Quaternary Selenides with Intriguing Structural Diversity and Nonlinear Optical Properties, Dalton Trans., 2016, 45, 7627-7633; (b) M. Y. Li, Y. X. Zhang, H. Lin, Z. J. Ma, X. T. Wu and Q. L. Zhu, Combined experimental and theoretical investigations of Ba₃GaS₄I: interesting structure transformation originated from the halogen substitution, Dalton Trans., 2019, 48, 17588-17593; (c) M. Y. Ran, Z. Ma, X. T. Wu, H. Lin and Q. L. Zhu, Ba₂Ge₂Te₅: a ternary NLOactive telluride with unusual one-dimensional helical chains and giant second-harmonic-generation tensors, Inorg. Chem. Front., 2021, 8, 4838-4845.
- 8 (a) A. Tudi, S. Han, Z. Yang and S. Pan, Potential optical functional crystals with large birefringence: Recent advances and future prospects, Coord. Chem. Rev., 2022, **459**, 214380; (b) Q. Shi, L. Dong and Y. Wang, Evaluating refractive index and birefringence of nonlinear optical crys-Classical methods and new developments, Chin. J. Struct. Chem., 2023, 42, 100017; (c) Y. Long, X. Dong, L. Huang, H. Zeng, Z. Lin, L. Zhou and G. Zou, BaSb(H₂PO₂)₃Cl₂: An Excellent UV Nonlinear Optical Hypophosphite Exhibiting Strong Second-Harmonic Generation Response, Mater. Today Phys., 2022, 28, 100876.
- 9 (a) H. Lin, Y. Y. Li, M. Y. Li, Z. J. Ma, L. M. Wu, X. T. Wu and Q. L. Zhu, Centric-to-acentric structure transformation induced by a stereochemically active lone pair: a new insight for design of IR nonlinear optical materials, J. Mater. Chem. C, 2019, 7, 4638-4643; (b) S. Han, A. Tudi, W. Zhang, X. Hou, Z. Yang and S. Pan, Recent Development of Sn(II), Sb(III)-based Birefringent Material: Crystal Chemistry and Investigation of Birefringence, Angew. Chem., Int. Ed., 2023, 62, e202302025; (c) C. Liu, S.-H. Zhou, C. Zhang, Y.-Y. Shen, X.-Y. Liu, H. Lin and Y. Liu, CsCu₃SbS₄: rational design of a two-dimensional layered material with giant birefringence derived from Cu₃SbS₄, Inorg. Chem. Front., 2022,

- (*d*) C. Zhang, M.-Y. Ran, X. Chen, S.-H. Zhou, H. Lin and Y. Liu, Stereochemically active lone-pair-driven giant enhancement of birefringence from three-dimensional CsZn₄Ga₅Se₁₂ to two-dimensional CsZnAsSe₃, *Inorg. Chem. Front.*, 2023, **10**, 3367–3374; (*e*) P.-F. Li, J.-G. Mao and F. Kong, A survey of stereoactive oxysalts for linear and nonlinear optical applications, *Mater. Today Phys.*, 2023, 37, 101197; (*f*) P.-F. Li, C.-L. Hu, J.-G. Mao and F. Kong, A UV Non-Hydrogen Pure Selenite Nonlinear Optical Material Achieving Balanced Properties through Framework-Optimized Structural Transformation, *Mater. Horiz.*, 2024, DOI: **10.1039/D3MH01790G**.
- 10 (a) X. Y. Zhang, X. G. Du, J. H. Wang, F. Y. Wang, F. Liang, Z. G. Hu, Z. S. Lin and Y. C. Wu, K₃C₆N₇O₃·2H₂O: A Multifunctional Nonlinear Optical Cyamelurate Crystal with Colossal π-Conjugated Orbitals, ACS Appl. Mater. Interfaces, 2022, 14, 53074–53080; (b) Y. Li, X. Zhang, J. Zheng, Y. Zhou, W. Huang, Y. Song, H. Wang, X. Song, J. Luo and S. Zhao, A Hydrogen Bonded Supramolecular Framework Birefringent Crystal, Angew. Chem., Int. Ed., 2023, 62, e202304498.
- 11 (a) J. Zhou, L. Wang, Y. Chu, H. Wang, S. Pan and J. Li, Na₃SiS₃F: A Wide Bandgap Fluorothiosilicate with Unique SiS₃F Unit and High Laser-Induced Damage Threshold, Adv. Opt. Mater., 2023, 11, 2300736; (b) M.-Y. Ran, S.-H. Zhou, W.-B. Wei, B.-X. Li, X.-T. Wu, H. Lin and Q.-L. Zhu, Breaking through the Trade-Off between Wide Band Gap and Large SHG Coefficient in Mercury-based Chalcogenides for IR Nonlinear Optical Application, Small, 2024, 20, 2304563; (c) A.-Y. Wang, S.-H. Zhou, M.-Y. Ran, X.-T. Wu, H. Lin and Q.-L. Zhu, Regulating the key performance parameters for Hg-based IR NLO chalcogenides via bandgap engineering strategy, Chin. Chem. Lett., 2024, 35, 109377; (d) P.-F. Li, Y.-P. Gong, C.-L. Hu, B. Zhang, J.-G. Mao and F. Kong, Four UV Transparent Linear and Nonlinear Optical Materials Explored from Pure Selenite Compounds, Adv. Opt. Mater., 2023, 11, 2301426.
- 12 (a) Y. F. Shi, W. Wei, X. T. Wu, H. Lin and Q. L. Zhu, Recent progress in oxychalcogenides as IR nonlinear optical materials, *Dalton Trans.*, 2021, **50**, 4112–4118; (b) J. J. Xu and K. Wu, Comprehensive review on multiple mixed-anion ligands, physicochemical performances and application prospects in metal oxysulfides, *Coord. Chem. Rev.*, 2023, **486**, 215139; (c) Y. Zhang, H. Wu, Z. Hu and H. Yu, Oxychalcogenides: A Promising Materials Class for Nonlinear Optical Crystals with Mixed-anion Groups, *Chem. Eur. J.*, 2022, **29**, e202203597; (d) J.-X. Zhang, P. Feng, M.-Y. Ran, X.-T. Wu, H. Lin and Q.-L. Zhu, *Coord. Chem. Rev.*, 2024, **502**, 215617.
- 13 (a) J. Guo, A. Tudi, S. Han, Z. Yang and S. Pan, Sn₂PO₄I: an excellent birefringent material with giant optical anisotropy in non π-conjugated phosphate, *Angew. Chem., Int. Ed.*, 2021, **60**, 24901–24904; (b) Y. Hu, C. Wu, X. Jiang, Z. Wang, Z. Huang, Z. Lin, X. Long, M. G. Humphrey and C. Zhang, Giant Second-Harmonic Generation Response and Large Band Gap in the Partially Fluorinated Mid-Infrared Oxide

- RbTeMo₂O₈F, *J. Am. Chem. Soc.*, 2021, **143**, 12455–12459; (c) Y. Deng, L. Huang, X. Dong, L. Wang, K. M. Ok, H. Zeng, Z. Lin and G. Zou, $K_2Sb(P_2O_7)F$: Cairo pentagonal layer with bifunctional genes reveal optical performance, *Angew. Chem., Int. Ed.*, 2020, **59**, 21151–21156.
- 14 R. Wang, F. Liang, X. Liu, Y. Xiao, Q. Liu, X. Zhang, L. M. Wu, L. Chen and F. Huang, Heteroanionic Melilite Oxysulfide: A Promising Infrared Nonlinear Optical Candidate with a Strong Second-Harmonic Generation Response, Sufficient Birefringence, and Wide Bandgap, ACS Appl. Mater. Interfaces, 2022, 14, 23645–23652.
- 15 (a) H. Lin, W. B. Wei, H. Chen, X. T. Wu and Q. L. Zhu, Rational design of infrared nonlinear optical chalcogenides by chemical substitution, *Coord. Chem. Rev.*, 2020, 406, 213150; (b) M. Y. Ran, A. Y. Wang, W. B. Wei, X. T. Wu, H. Lin and Q. L. Zhu, Recent progress in the design of IR nonlinear optical materials by partial chemical substitution: structural evolution and performance optimization, *Coord. Chem. Rev.*, 2023, 481, 215059; (c) H. D. Yang, M. Y. Ran, W. B. Wei, X. T. Wu, H. Lin and Q. L. Zhu, Recent advances in IR nonlinear optical chalcogenides with well-balanced comprehensive performance, *Mater. Today Phys.*, 2023, 35, 101127.
- 16 Y. Shi, Z. Ma, B. Li, X. Wu, H. Lin and Q. Zhu, Phase matching achieved by isomorphous substitution in IR non-linear optical material Ba₂SnSSi₂O₇ with an undiscovered [SnO₄S] functional motif, *Mater. Chem. Front.*, 2022, **6**, 3054–3061.
- 17 M. Sun, W. Xing, M. Lee and J. Yao, Bridging oxygen atoms in trigonal prism units driven strong second-harmonic-generation efficiency in Sr₃Ge₂O₄Te₃, *Chem. Commun.*, 2022, **58**, 11167–11170.
- 18 M. Y. Ran, S. H. Zhou, B. Li, W. Wei, X. T. Wu, H. Lin and Q. L. Zhu, Enhanced Second-Harmonic-Generation Efficiency and Birefringence in Melilite Oxychalcogenides Sr₂MGe₂OS₆ (M = Mn, Zn, and Cd), *Chem. Mater.*, 2022, 34, 3853–3861.
- 19 M. Ozima, J. Susaki, S. Akimoto and Y. Shimizu, The system BaOGeO₂ at high pressures and temperatures, with special reference to high-pressure transformations in BaGeO₃, BaGe₂O₅, and Ba₂Ge₅O₁₂, *J. Solid State Chem.*, 1982, 44, 307–317.
- 20 (a) J. Xu, Y. Xiao, K. Wu, B. Zhang, D. Lu, H. Yu and H. Zhang, Flexible Anionic Groups-Activated Structure Dissymmetry for Strong Nonlinearity in Ln₂Ae₃M^{IV}₃S₁₂ Family, *Small*, 2024, 20, 2306577; (b) Y. Huang, Y. Zhang, D. Chu, Z. Yang, G. Li and S. Pan, HgB₂S₄: A d¹⁰ Metal Thioborate with Giant Birefringence and Wide Band Gap, *Chem. Mater.*, 2023, 35, 4556–4563; (c) G. Li, Z. Yang, X. Hou and S. Pan, Chain-like [S_x] (x = 2–6) Units Realizing Giant Birefringence with Transparency in the Near-Infrared for Optoelectronic Materials, *Angew. Chem., Int. Ed.*, 2023, 62, e202303711.
- 21 J. Xu, K. Wu, Y. Xiao, B. Zhang, H. Yu and H. Zhang, Mixed-AnionOriented Design of LnMGa₃S₆O (Ln = La, Pr, and Nd; M = Ca and Sr) Nonlinear Optical Oxysulfides with

- Targeted Property Balance, ACS Appl. Mater. Interfaces, 2022, 14, 37967–37974.
- 22 (a) N. Zhang, Q. Xu, Z. Shi, M. Yang and S. Guo, Characterizations and Nonlinear-Optical Properties of Pentanary Transition-Metal Oxysulfide Sr₂CoGe₂OS₆, *Inorg. Chem.*, 2022, **61**, 17002–17006; (b) H. D. Yang, S. H. Zhou, M. Y. Ran, X. T. Wu, H. Lin and Q. L. Zhu, Melilite oxychalcogenide Sr₂FeGe₂OS₆: a phase-matching IR nonlinear optical material realized by isomorphous substitution, *Inorg. Chem. Front.*, 2023, **10**, 2030.
- 23 W. Xing, P. Fang, N. Wang, Z. Li, Z. Lin, J. Yao, W. Yin and B. Kang, Two Mixed-Anion Units of [GeOSe₃] and [GeO₃S] Originating from Partial Isovalent Anion Substitution and Inducing Moderate Second Harmonic Generation Response and Large Birefringence, *Inorg. Chem.*, 2020, 59, 16716–16724.
- 24 M. Sun, W. Xing, M. Lee and J. Yao, Bridging oxygen atoms in trigonal prism units driven strong second-harmonic-generation efficiency in Sr₃Ge₂O₄Te₃, *Chem. Commun.*, 2022, 58, 11167–11170.
- 25 (a) X. Zhang, Y. Xiao, R. Wang, P. Fu, C. Zheng and F. Huang, Synthesis, crystal structures and optical properties of noncentrosymmetric oxysulfides AeGeS₂O (Ae = Sr, Ba), *Dalton Trans.*, 2019, 48, 14662–14668; (b) H. Yang, S. Zhou, M. Ran, X. Wu, H. Lin and Q. Zhu, Oxychalcogenides as Promising Ultraviolet Nonlinear Optical Candidates: Experimental and Theoretical Studies of AEGeOS₂ (AE = Sr and Ba), *Inorg. Chem.*, 2022, 61, 15711–15720.
- 26 (a) M. Y. Ran, Z. J. Ma, H. Chen, B. X. Li, X. T. Wu, H. Lin and Q. L. Zhu, Partial Isovalent Anion Substitution to Access Remarkable Second-Harmonic Generation Response: A Generic and Effective Strategy for Design of Infrared Nonlinear Optical Materials, *Chem. Mater.*, 2020, 32, 5890–5896; (b) B. Liu, X. Jiang, G. Wang, H. Zeng, M. Zhang, S. Li, W. Guo and G. Guo, Oxychalcogenide BaGeOSe₂: Highly Distorted Mixed-Anion Building Units Leading to a Large Second-Harmonic Generation Response, *Chem. Mater.*, 2015, 27, 8189–8192.
- 27 H. Liu, Z. Song, H. Wu, Z. Hu, J. Wang, Y. Wu and H. Yu, [Ba₂F₂][Ge₂O₃S₂]: An Unprecedented Heteroanionic Infrared Nonlinear Optical Material Containing Three Typical Anions, ACS Mater. Lett., 2022, 4, 1593–1598.
- 28 C. A. Niedermeier, J.-I. Yamaura, J. Wu, X. He, T. Katase, H. Hosono and T. Kamiya, Crystal Structure Built from a GeO_6 – GeO_5 Polyhedra Network with High Thermal Stability: β – $SrGe_2O_5$, ACS Appl. Electron. Mater., 2019, 1, 1989–1993.
- 29 S. H. Zhou, M. Y. Ran, W. Wei, A. Y. Wang, X. T. Wu, H. Lin and Q. L. Zhu, Heteroanion-introduction-driven birefringence enhancement in oxychalcogenide Ba₃M^{II}Ge₃O₂S₈ (M^{II} = Mn, Cd), *Inorg. Chem. Front.*, 2023, **10**, 5997–6004.
- 30 (a) Z. Li, S. Zhang, Z. Huang, L.-D. Zhao, E. Uykur, W. Xing, Z. Lin, J. Yao and Y. Wu, Molecular Construction from AgGaS₂ to CuZnPS₄: Defect-Induced Second Harmonic Generation Enhancement and Cosubstitution-Driven Band

- Gap Enlargement, *Chem. Mater.*, 2020, **32**, 3288–3296; (*b*) M.-Y. Li, Z. Ma, B. Li, X.-T. Wu, H. Lin and Q.-L. Zhu, HgCuPS₄: An Exceptional Infrared Nonlinear Optical Material with Defect Diamond-like Structure, *Chem. Mater.*, 2020, **32**, 4331–4339; (*c*) Y. Chu, P. Wang, H. Zeng, S. Cheng, X. Su, Z. Yang, J. Li and S. Pan, Hg₃P₂S₈: A New Promising Infrared Nonlinear Optical Material with a Large Second-Harmonic Generation and a High Laser-Induced Damage Threshold, *Chem. Mater.*, 2021, **33**, 6514–6521.
- 31 (a) P. Kubelka, Ein beitrag zur optik der farbanstriche, J. Tech. Phys., 1931, 12, 593; (b) M. A. Butler, Photoelectrolysis and physical properties of the semiconducting electrode WO₂, J. Appl. Phys., 1977, 48, 1914.
- 32 (a) Y. Wang, M. Luo, P. Zhao, X. Che, Y. Cao and F. Huang, Sr₄Pb_{1.5}Sb₅O₅Se₈: a new mid-infrared nonlinear optical material with a moderate SHG response, CrystEngComm, 2020, 22, 3526-3530; (b) R. Wang, F. Wang, X. Zhang, X. Feng, C. Zhao, K. Bu, Z. Zhang, T. Zhai and F. Q. Huang, Improved Polarization in the Sr₆Cd₂Sb₆O₇Se₁₀ Oxyselenide through Design of Lateral Sublattices for Efficient Photoelectric Conversion, Angew. Chem., Int. Ed., 2022, 61, e202206816; (c) R. Wang, F. Liang, X. Zhang, Y. Yang and F. Huang, Synthesis, structural evolution and optical properties of a new family of oxychalcogenides [Sr₃VO₄][MQ₃][M = Ga, In, Q = S, Se), Inorg. Chem. Front., 2022, 9, 4768-4775; (d) J. K. Wang, Y. S. Cheng, H. P. Wu, Z. G. Hu, J. Y. Wang, Y. C. Wu and H. W. Yu, Sr₃[SnOSe₃][CO₃]: A Heteroanionic Nonlinear Optical Material Containing Planar p-conjugated [CO₃] and Heteroleptic [SnOSe₃] Anionic Groups, Angew. Chem., Int. Ed., 2022, 61, e202201616.
- 33 Y. X. Chen, Z. X. Chen, Y. Zhou, Y. Q. Li, Y. C. Liu, Q. R. Ding, X. Chen, S. G. Zhao and J. H. Luo, An Antimony (III) Fluoride Oxalate With Large Birefringence, *Chem. Eur. J.*, 2021, 27, 4557–4560.
- 34 M. J. Dodge, Refractive properties of magnesium fluoride, *Appl. Opt.*, 1984, 23, 1980–1985.
- 35 D. E. Zelmon, D. L. Small and D. Jundt, Infrared corrected Sellmeier coefficients for congruently grown lithium niobate and 5 mol% magnesium oxide-doped lithium niobate, *J. Opt. Soc. Am. B*, 1997, 14, 3319–3322.
- 36 K. Ding, H. Wu, Z. Hu, J. Wang, Y. Wu and H. Yu, [Ba₄(S₂)][ZnGa₄S₁₀]: Design of an Unprecedented Infrared Nonlinear Salt-Inclusion Chalcogenide with Disulfide-Bonds, *Small*, 2023, **19**, 2302819.
- 37 Y. Yun, M. Wu, C. Xie, Z. Yang, G. Li and S. Pan, Theoretical Prediction-Assisted Synthesis and Characterization of Infrared Nonlinear Optical Material NaSrBS₃, *Adv. Opt. Mater.*, 2023, **11**, 2300256.
- 38 X. Ji, H. Wu, B. Zhang, H. Yu, Z. Hu, J. Wang and Y. Wu, Intriguing Dimensional Transition Inducing Variable Birefringence in K₂Na₂Sn₃S₈ and Rb₃NaSn₃Se₈, *Inorg. Chem.*, 2021, **60**, 1055–1061.
- 39 P. E. Blochl, Projector augmented-wave method, *Phys. Rev. B: Condens. Matter*, 1994, **50**, 17953–17979.
- 40 (a) R. Wang, F. Liang, F. Wang, Y. Guo, X. Zhang, Y. Xiao, K. Bu, Z. Lin, J. Yao, T. Zhai and F. Huang, Sr₆Cd₂Sb₆O₇S₁₀:

This article is licensed under a Creative Commons Attribution-NonCommercial 3.0 Unported Licence.

Strong SHG Response Activated by Highly Polarizable Sb/ O/S Groups, Angew. Chem., Int. Ed., 2019, 58, 8078-8081; (b) M. Y. Ran, S. H. Zhou, W. Wei, B. Li, X. T. Wu, H. Lin and Q. L. Zhu, Rational Design of a Rare-Earth Oxychalcogenide Nd₃[Ga₃O₃S₃][Ge₂O₇] with Superior Infrared Nonlinear Optical Performance, Small, 2023, 19, 2300248; (c) J. N. Li, X. H. Li, Y. X. Xu, W. L. Liu and S. P. Guo, First Investigation of Nonlinear Optical Oxychalcogenide with Three-Dimensional Anionic

Framework and Special Windmill-Like Functional Motifs, Chin. J. Chem., 2022, 40, 2407-2414; (d) Y. Cheng, H. Wu, H. Yu, Z. Hu, J. Wang and Y. Wu, Rational Design of a Promising Oxychalcogenide Infrared Nonlinear Optical Crystal, Chem. Sci., 2022, 13, 5305-5310; (e) Y. Shi, S. Zhou, P. Liu, X. Wu, H. Lin and Q. Zhu, Unique $[Sb_6O_2S_{13}]^{12-}$ finite chain in oxychalcogenide Ba₆Sb₆O₂S₁₃ leading to ultra-low thermal conductivity and giant birefringence, Inorg. Chem. Front., 2023, 10, 4425-4434.